Chaos, Solitons and Fractals 41 (2009) 2201–2215

Contents lists available at ScienceDirect

Chaos, Solitons and Fractals

journal homepage: www.elsevier.com/locate/chaos

Clustering and diffusion in a symplectic map lattice with non-local coupling

C.F. Woellner [a], S.R. Lopes [a], R.L. Viana [a,*], I.L. Caldas [b]

[a] Departamento de Física, Universidade Federal do Paraná, Caixa Postal 19044, 81531-990 Curitiba, Paraná, Brazil
[b] Instituto de Física, Universidade de São Paulo, Caixa Postal 66318, 05315-970 São Paulo, SP, Brazil

ARTICLE INFO

Article history:
Accepted 19 August 2008

ABSTRACT

We study a symplectic chain with a non-local form of coupling by means of a standard map lattice where the interaction strength decreases with the lattice distance as a power-law, in such a way that one can pass continuously from a local (nearest-neighbor) to a global (mean-field) type of coupling. We investigate the formation of map clusters, or spatially coherent structures generated by the system dynamics. Such clusters are found to be related to stickiness of chaotic phase-space trajectories near periodic island remnants, and also to the behavior of the diffusion coefficient. An approximate two-dimensional map is derived to explain some of the features of this connection.

1. Introduction

The standard map (SM), also called Chirikov–Taylor map, besides being a paradigmatic dynamical system, describes a variety of situations of physical interest [1]. It is a two-dimensional area-preserving map $p \mapsto p' = p + (K/2\pi)\sin(2\pi x)$, $x \mapsto x' = x + p', (\mathrm{mod}\ 1)$, where K is a measure of the non-linearity of the system, and (p, x) are canonical variables which may play different roles as this map is used in physical applications.

In plasma physics, the SM models the interaction between a charged particle and an electrostatic plane wave train [2,3], the behavior of drift orbits in tokamaks in the presence of drift waves [4]; and it is useful as a lowest-order description of the magnetic-field line structure in plasma confinement systems [5]. In accelerator physics, SM describes the interaction of a charged particle in a cyclotron under the influence of a periodic potential applied to a small region [6]. In optics, the SM was found to characterize the chaotic evolution of the polarization in optical fibers with modulated birefringence [7]. The quantum periodically kicked rotator, the classical limit of which is described by the SM, is one of the most intensively investigated models of quantum chaos [8].

Since the SM is widely used as a paradigmatic system for studying Hamiltonian dynamics, chains of coupled SM can be considered as representative examples of volume-preserving and spatially extended systems. A physically interesting example would be a chain of coupled driven rotators, for which the coupling is modulated through a sequence of delta-pulsed kicks. One possible realization consists of an array of pendula with coils on them. If a short current pulse flows through the coils, the interaction force among the pendula will act during a short time interval and thus can be approximated with a delta function [9].

Lattices of locally coupled SM, for which each map interacts with their nearest-neighbors, have been studied as models of higher-dimensional Hamiltonian systems. Unlike the isolated SM, for which the dynamics is fairly well-understood due to standard mathematical results like Poincaré-Birkhoff and KAM theorems [10], systems of coupled SM exhibit a far more complex dynamics, since KAM tori no longer divide the phase-space and thus the whole chaotic layer can be connected, generating phenomena like Arnold diffusion [1]. Since Arnold diffusion is extremely slow [11,12], the timescale in which we have to work turns to be too large to allow the use of perturbative approaches. Kaneko and Konishi shown

* Corresponding author.
E-mail address: viana@fisica.ufpr.br (R.L. Viana).

0960-0779/$ - see front matter © 2008 Elsevier Ltd. All rights reserved.
doi:10.1016/j.chaos.2008.08.026

that, in locally coupled SM lattices, anomalous diffusion exists only up to a crossover time, beyond which the diffusion becomes of a Gaussian nature [13,14]. This was explained by the fast decay of the spatial correlations over the lattice, such that the number of degrees of freedom relevant to diffusion is considerably less than the lattice size. Hence in the thermodynamic limit the system exhibits size independence and intensive behavior. Diffusion in phase-space was also investigated for globally coupled SM lattices [15,16]. There has been found extensive behavior in the limit of a strongly chaotic regime in such a way that, within this global regime, the spatial correlations are negligible and the diffusion is size-dependent.

Gyorgyi and coworkers have shown that the measure of the system phase-space occupied by periodic islands *versus* that occupied by chaotic trajectories decays rapidly with the number of coupled maps [17]. If the number of degrees of freedom (which, in a coupled SM lattice, is twice the number of maps) is too large, the characteristics of diffusion are expected to depend largely on the measure occupied by chaotic orbits, which turns to be extremely difficult to evaluate directly. Hence we must resort to indirect methods to evaluate the measure of the phase-space occupied by chaotic orbits, like the Lyapunov spectrum and the metric (Kolmogorov–Sinai) entropy.

In order to put into a unified framework both local (nearest-neighbor) and global (mean-field) coupling schemes, we introduced a non-local coupling prescription where a given site interacts with all neighbors, the corresponding strength decaying with the lattice in a power-law fashion. In this paper, we analyze the dependence of the Lyapunov spectrum and entropy on the coupling parameters, namely the strength and effective range. Our results show different scaling behaviors with coupling strength and range, which are compatible with phase-space changes observed in the numerically obtained Poincaré maps.

The dynamics generated by SM coupled lattices, although being chiefly chaotic, also presents a dependence on remnants of periodic islands embedded in the chaotic phase-space region [18]. This dependence is manifested in the so-called stickiness effect, which makes chaotic trajectories to spend a typically long time in the vicinity of the periodic island remnants, with a non-exponentially small probability. The sticky trajectory segments are also called flights [19], which can be studied by means of finite-time Lyapunov exponents [20]. If we consider a finite-time interval a chaotic orbit with stickiness can be viewed as a dynamical trap, which affects the transport properties characteristic of chaotic motion [21]. In particular, the diffusion is considerably reduced in comparison with a uniformly hyperbolic chaotic region [22].

There are other detectable effects of stickiness in lattices of coupled SM, like the formation of map clusters, which represent spatially coherent regions with similar temporal evolutions. Clustering in symplectic map lattices has been described in globally coupled SM by Konishi and Kaneko [15], who also revealed their finite lifetime and fractal geometric structure. For general dissipative coupled map lattices, clustering is related to the formation of one or more synchronized patterns, and is a typical feature of global couplings [23]. In this paper, we present numerical evidence that clustering is an observable manifestation of stickiness in coupled symplectic map lattices. Cluster formation through stickiness of chaotic trajectories is closely related to the coupling properties, and this effect is enhanced as the coupling becomes more of a global nature. Some aspects of the relation between clustering and stickiness are revealed through an approximate two-dimensional map.

The rest of the paper is organized as follows: in Section 2, we introduce the coupled map lattice model and some of its properties. The Lyapunov spectrum and the corresponding entropy for this model are shown in Section 3. Section 4 analyzes cluster formation and the stickiness of chaotic trajectories. Section 5 considers phase-space diffusion, whereas in Section 6 we explore some properties of an approximate two-dimensional map describing the dynamics in the vicinity of island centers, in order to explain some features of stickness. The last section contains our conclusions.

2. Map lattice with non-local coupling

Let us consider a one-dimensional lattice of N sites, each of them with two state variables at discrete time n : $p_n^{(i)}$ and $x_n^{(i)}$, where $i = 1, 2, \ldots N$ runs over the lattice sites. The time evolution at each site is governed by the SM, modified by the non-local coupling with the other sites, and given by Rogers and Wille [24]

$$p_{n+1}^{(i)} = p_n^{(i)} + \frac{K}{2\pi\sqrt{\eta(\alpha)}} \sum_{j=1}^{N'} \frac{1}{j^{\alpha}} \left\{ \sin\left[2\pi(x_n^{(i+j)} - x_n^{(i)})\right] + \sin\left[2\pi(x_n^{(i-j)} - x_n^{(i)})\right] \right\}, \tag{1}$$

$$x_{n+1}^{(i)} = x_n^{(i)} + p_{n+1}^{(i)}, \tag{2}$$

where $x \in [-1/2, +1/2], N' = (N-1)/2$, with N odd; and $K > 0$ plays the double role of being the coupling strength and the non-linearity parameter. Hence the isolated SM does not follow from the $K \to 0$ limit in Eq. (1).

The coupling is non-local because the summation in (1) runs over all the neighbors of a given site, but the intensity of the coupling decays with the lattice distance as a power-law, the corresponding normalization factor being

$$\eta(\alpha) = 2 \sum_{j=1}^{N'} \frac{1}{j^{\alpha}}. \tag{3}$$

The parameter $\alpha > 0$ represents the effective range of the interaction in such a way that, on varying α, we can pass continuously from a global to a local type of coupling.

Let us consider the two limiting cases of this coupling prescription. If we take $\alpha \to \infty$, there follows that all values of j would give vanishing contributions to the coupling term, except the case $j = 1$. Accordingly, we have that $\eta \to 2$, and our coupling reduces to a local, or Laplacian form

$$p_{n+1}^{(i)} = p_n^{(i)} + \frac{K}{2\pi\sqrt{2}}\{\sin\left[2\pi(x_n^{(i+1)} - x_n^{(i)})\right] + \sin\left[2\pi(x_n^{(i-1)} - x_n^{(i)})\right]\}, \tag{4}$$

$$x_{n+1}^{(i)} = x_n^{(i)} + p_{n+1}^{(i)}, \tag{5}$$

in which a given site interacts only with its nearest-neighbors. Apart from the unessential factor $\sqrt{2}$, this is the type of coupling used in Ref. [13].

In the $\alpha \to 0$ limit of Eqs. (1) and (2), we have $\eta = 2N' = N - 1$ and the strength of interaction is the same for all neighbors of a given site, making for a "mean-field" global type of coupling:

$$p_{n+1}^{(i)} = p_n^{(i)} + \frac{K}{2\pi\sqrt{N-1}}\sum_{j=1, j\neq i}^{N}\sin\left[2\pi(x_n^{(j)} - x_n^{(i)})\right], \tag{6}$$

$$x_{n+1}^{(i)} = x_n^{(i)} + p_{n+1}^{(i)}, \tag{7}$$

which was used in Ref. [14]. We also mention that Gyorgyi et al. have used a different form of global coupling, in which the coupling term is separated from the non-linearity of the isolated map [17].

Eqs. (1) and (2) represent a volume-preserving dynamical system in the $2N$-dimensional phase-space, i.e., the Jacobian determinant is equal to the unity and the symplectic area

$$\sum_{i=1}^{N} \mathrm{d}p_n^{(i)} \wedge \mathrm{d}x_n^{(i)} = \sum_{i=1}^{N} \mathrm{d}p_{n+1}^{(i)} \wedge \mathrm{d}x_{n+1}^{(i)}, \tag{8}$$

where $\wedge$ denotes the exterior product, is conserved with respect to the time evolution of the system. Consequently, we can write down an explicit time-dependent Hamiltonian for this system, which reads

$$H = \frac{1}{2}\sum_{i=1}^{N}[p^{(i)}]^2 - \frac{K}{(2\pi)^2\sqrt{\eta(\alpha)}}\cdot\sum_{i=1}^{N}\sum_{j=1}^{N'}\frac{1}{j^{\alpha}}\{\cos\left[2\pi(x_n^{(i+j)} - x_n^{(i)})\right] + \cos\left[2\pi(x_n^{(i-j)} - x_n^{(i)})\right]\}\sum_{n=-\infty}^{+\infty}\delta(t-n), \tag{9}$$

in such a way that the continuous-time limit of the map equations yields the canonical equations

$$\frac{\mathrm{d}p^{(i)}}{\mathrm{d}t} = -\frac{\partial H}{\partial x^{(i)}}, \tag{10}$$

$$\frac{\mathrm{d}x^{(i)}}{\mathrm{d}t} = \frac{\partial H}{\partial p^{(i)}}. \tag{11}$$

Besides the symplectic area, the system given by Eqs. (1) and (2) also preserves the total momentum

$$\sum_{i=1}^{N} p_{n+1}^{(i)} = \sum_{i=1}^{N} p_n^{(i)} = \text{const.}, \tag{12}$$

such that the phase-space trajectories lie on a $(2N-2)$-dimensional hyper-plane.

In the numerical simulations we choose random initial conditions $(x_0^{(i)}, p_0^{(i)})$ and periodic boundary conditions $(x_n^{(i\pm N)}, p_n^{(i\pm N)}) = (x_n^{(i)}, p_n^{(i)})$ for a lattice of $N = 25$ maps. Due to the coupling between sites for $K \neq 0$, trajectories are free to move through a 48-dimensional phase-space since invariant tori no longer divide the energetically available region. Two-dimensional projections of the phase-space, $(x^{(i)}, p^{(i)})$, typically show a large number of orbits which encircle marginally stable points lying on the line $p = 0$ (Fig. 1).

In order to compare such orbits with those expected for an *isolated* SM, in Fig. 2(a) we depict a phase portrait (p_n *versus* x_n) for an isolated SM with $K = 0.5$. The latter has fixed points at $(p, x) = (0, 0)$ and $(0, \pm 1/2)$, which are, respectively, a center and a hyperbolic saddle. Since K is non-zero we have thin regions of chaotic dynamics due to non-integrability. In particular, for $K > K_c \approx 1$ all the invariant tori are broken down and a wide chaotic region begins to show up, allowing for large excursions of the p-variable [Fig. 2(c)].

These results are to be compared with Fig. 2(b) and (d), where we choose one of the coupled maps, say $i = 10$, and show 5,000 points of a same trajectory in the corresponding phase-space projection ($p_n(10)$ *versus* $x_n(10)$), with the same values of K as from Fig. 2(a) and (c). For small K [Fig. 2(b)] the origin of the chosen projection now is a non-linear center, surrounded by some tori. Other projections, however, would show different features since the coupled system mixes up the dynamics of all sites. A higher value of K, on the other hand, leaves an almost totally chaotic region [Fig. 2(b)].

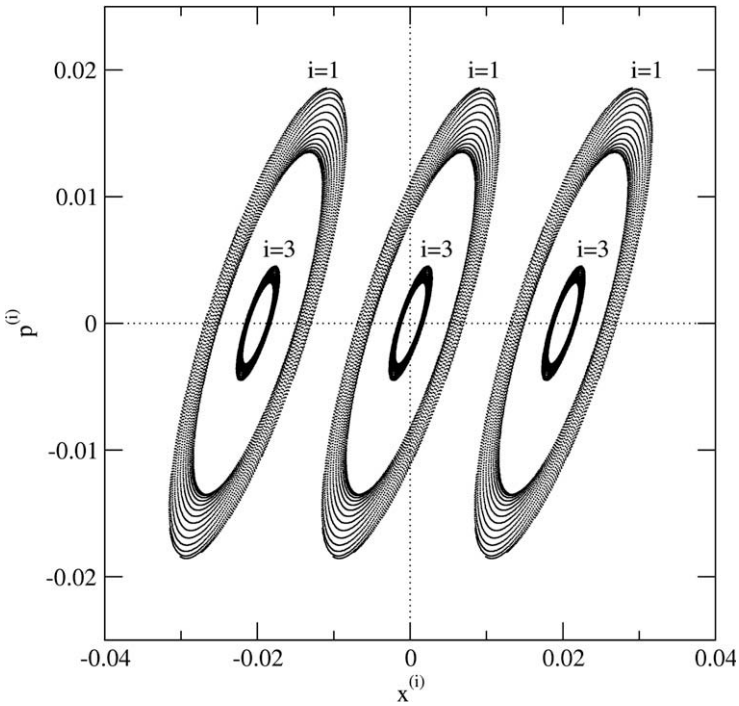

Fig. 1. Phase-space projections $p^{(i)} - x^{(i)}$ for sites $i = 1$ and $i = 3$ showing some orbits encircling marginally stable points on the line $p = 0$ for the coupled SM lattice with $\alpha = 0.0$ and $K = 0.5$.

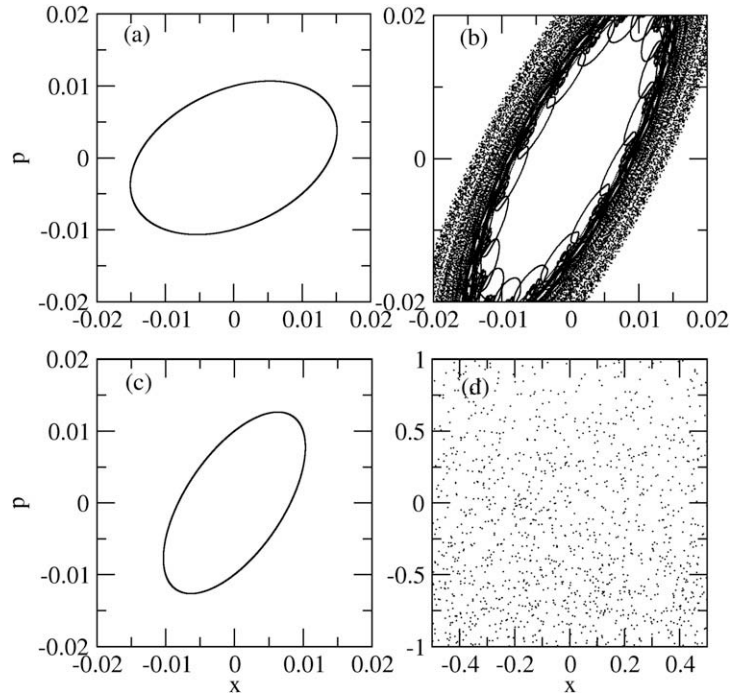

Fig. 2. Phase plane for an isolated standard map with (a) $K = 0.5$ and (c) $K = 1.5$. Phase-space projection $p^{(10)}$ *versus* $x^{(10)}$ for (b) $K = 0.5$ and (d) $K = 1.5$. A single trajectory with 5000 points is shown with initial conditions $x_0^{(10)} = -0.004864$ and $p_0^{(10)} = -0.003857$.

In general we expect such a wide chaotic region with a few tori interspersed, such that large-scale excursions occur with diffusion in the action variable.

3. Lyapunov spectrum

A lattice with N coupled two-dimensional maps is a $2N$-dimensional dynamical system, and the corresponding Lyapunov spectrum has $2N$ exponents, one for each independent eigendirection in the tangent space: $\lambda_1 = \lambda_{\max} > \lambda_2 > \ldots > \lambda_{2N}$. Since the coupled map lattice (1) and (2) preserves phase-space volumes, the sum of all exponents vanishes:

$$\sum_{i=1}^{2N} \lambda_i = 0. \tag{13}$$

In fact, it turns out that the exponent cancel in pairs, $\lambda_{N+i} = -\lambda_{N-i+1}$ for $i = 1, 2, \ldots 2N$, such that $\lambda_N = \lambda_{N+1} = 0$ and the spectrum is symmetric.

Representative examples of the Lyapunov spectrum are depicted in Fig. 3, where the Lyapunov exponents for a lattice of $N = 25$ coupled maps (1) and (2) are shown for two coupling strengths and different values of the range parameter. When K takes on a small value [Fig. 3(a)] the spectrum is practically the same for all values of α but $\alpha = 0$ (the global mean-field case), for which the absolute values of the Lyapunov exponents are larger than for the other cases. This can be regarded as a consequence of the long-ranging interactions which occurs in global couplings thanks to the number and intensity of the connections (all sites interact mutually with equal intensity). Local couplings, on the other hand, have a short interaction range and thus a weaker lattice diffusion, thus diminishing the absolute value of the Lyapunov exponents. For larger K [Fig. 3(b)] these observations remain valid, but there are more differences among the spectra for local couplings.

In the spectra shown in Fig. 3 many Lyapunov exponents are positive, hence a quantity of interest is the lattice-averaged value of the positive Lyapunov exponents [25]

$$h = \frac{1}{N} \sum_{i=1}^{\lambda_i > 0} \lambda_i, \tag{14}$$

which is related to the area under the curve of the spectra of Fig. 3. According to Pesin's formula, if certain necessary conditions apply, the quantity h equals the density of Kolmogorov–Sinai (KS) entropy [26]. However, this equality holds rigorously only if the system would possess a SRB (Sinai–Ruelle–Bowen) measure, which is continuous along unstable directions of periodic orbits [27]. Such measures are known only for a few map lattices [28] but, in spite of this, h turns to be useful as a measure of the chaotic instability in the system phase-space, i.e., the growth rate related to the expanding eigendirections. Due to the volume-preservation, $-h$ is thus the shrinking rate related to the contracting eigendirections.

We averaged the entropy density over a number of different initial patterns, and analyze its dependence on the coupling strength ϵ and effective range α. Fig. 4 shows a plot of $\langle h \rangle$ *versus* K for different values of the range parameter. In all cases

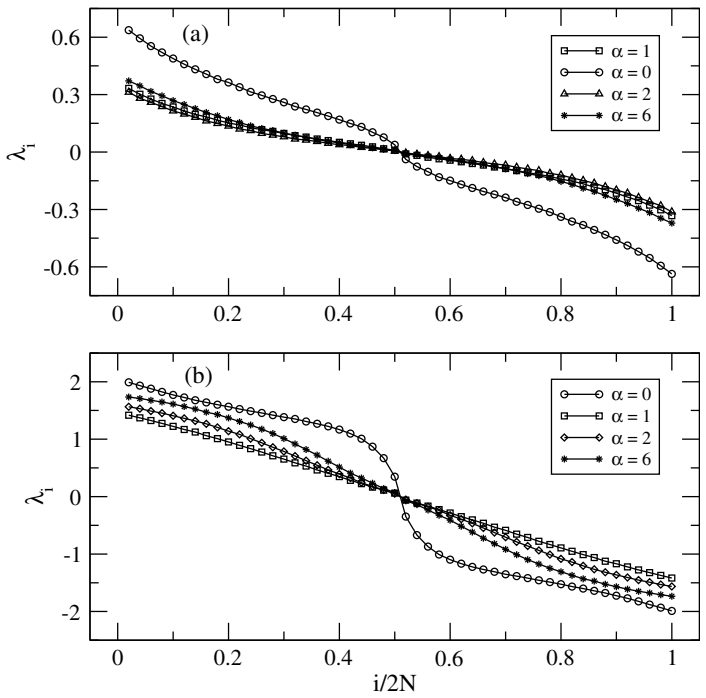

Fig. 3. Spectrum of the Lyapunov exponents for a lattice of $N = 25$ coupled standard maps with (a) $K = 0.7$; (b) $K = 5.0$.

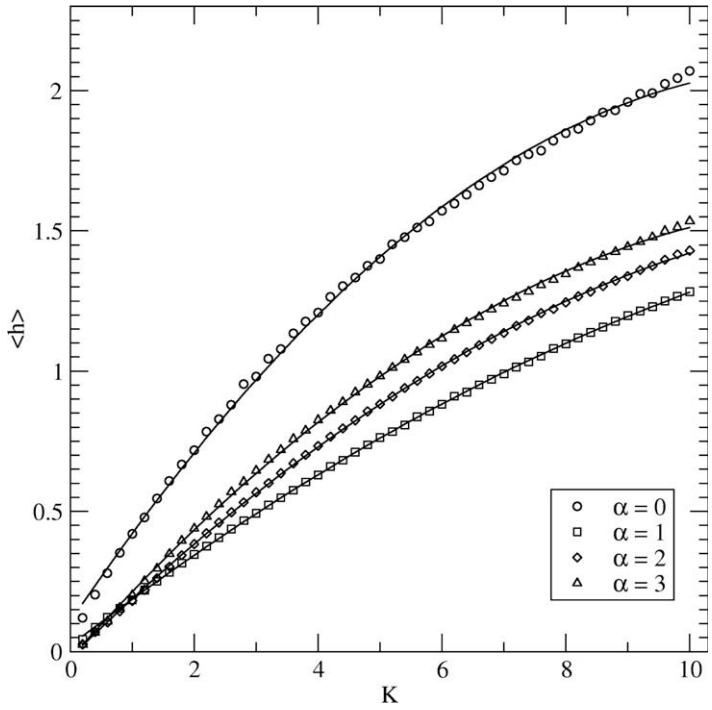

Fig. 4. Density of KS-entropy for a lattice of $N = 25$ coupled standard maps *versus* coupling strength for different values of the range parameter. The solid curves are least-squares fits.

considered the averaged entropy density increases monotonically with K; the numerical results being well-fitted by quadratic functions $\langle h\rangle \sim a_1 K - a_2 K^2$, with $0.1 \lesssim a_1 \lesssim 0.3$ and $a_2 \sim 10^{-2}$. The $\alpha = 0$ case bears the largest values of the entropy for a fixed K, as we have just discussed. Moreover, if K is small the differences of $\langle h\rangle$ among distinct values of α are small, and increase as K builds up, in agreement with Fig. 3.

There is another feature of interest here, and which also follows from the results depicted in Fig. 5, where the average entropy is plotted against the range parameter. For a given K-value, the entropy takes on a maximum value for $\alpha = 0$; then

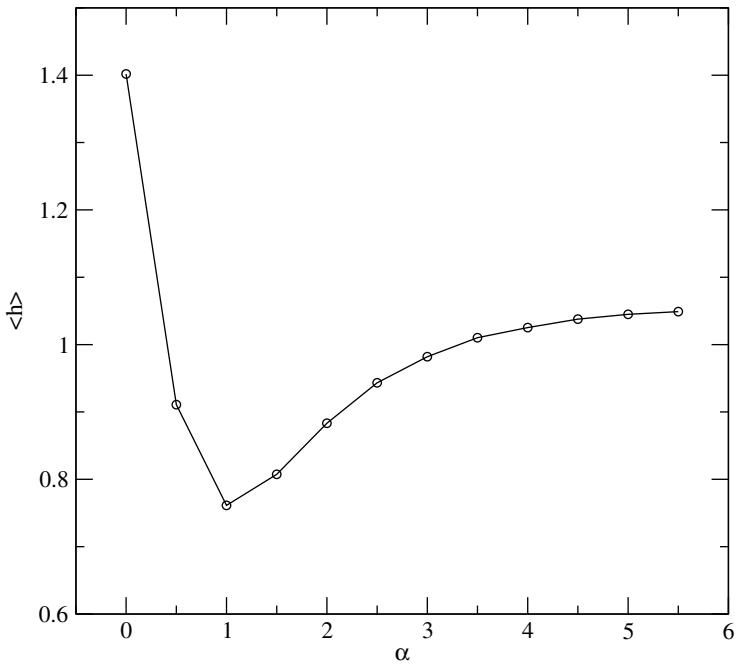

Fig. 5. Density of KS-entropy for a lattice of $N = 25$ coupled standard maps *versus* range parameter for $K = 5.0$.

decreases to a minimum for $\alpha = 1$ and increases again for higher values of α, but never to achieve the value it had before for $\alpha = 0$. The reason for this non-monotonic behavior with α lies in the intricacies of the spatio-temporal dynamics of the coupled system, but we can make some guesses based on previous facts known for certain dissipative map lattices with coupling prescription similar to that used in the present work.

In lattices of coupled chaotic piecewise linear and logistic maps at outer crisis, there was observed a transition from synchronized to non-synchronized behavior for $\alpha \approx 1$ [29]. For the globally dissipative systems obtained for $0 < \alpha \lesssim 1$ the synchronized attractor lies in a low-dimensional manifold in the phase-space, thus yielding a dramatic dimensional reduction. The entropy density, being divided by the number of positive exponents (just one positive exponent along the synchronization manifold), turns out to be very small for synchronized states. A SM lattice cannot exhibit synchronized motion, but we have observed a kind of coherent behavior for α near unity, which bears some similarities with synchronized states. The entropy decreases as we achieve these coherent states even though there is no dimensional reduction at all due to the symplectic nature of the coupled lattice. Moreover, the chaotic instability is reduced due to a dynamical effect named stickiness, which occurs for the chaotic regime in the neighborhood of remnant periodic islands. Both situations are to be quantitatively discussed in the next section.

4. Clustering and stickiness

The symplectic nature of the coupled map lattice treated in this paper prevents it from having attractors in phase-space, and synchronization of chaos is thus impossible to attain, at least in its original sense. We observe, however, spatio-temporal patters which, if not synchronized at all, do present coherent dynamics related to the formation of clusters of chaotic trajectories in the high-dimensional phase-space of the coupled map lattice. Such clusters are characterized by similar, yet not equal, values of the position variable. More precisely, in a M-cluster a given number M of coupled maps satisfy

$$|x_n^{(i)} - x_n^{(j)}| < C, \tag{15}$$

where $i, j = 1, 2, \ldots M \leqslant N$ and $C \ll |x_n^{(i)}|$ is a small tolerance level. Notice that no mention is made to the momentum variables in the definition above, which means that we consider clustered states one or more rotors with similar values of their angular position, regardless of their momenta. If we regard the maps as describing particles in a one-dimensional chain, clustered states would correspond to localized bunches of particles which may or may not have different velocities. Using periodic boundary conditions, we may think of those particles as initially randomly distributed along a unit circle, and they gradually move together to form a cluster, in which the particles show mutually oscillatory behavior.

Hence a clustered state is not a synchronized state of the system, since only half of the phase variables are considered. Moreover, due to the symplectic property there is no attracting state for trajectories, and hence no synchronization manifold can be defined for such a system. Nevertheless, since clustered states in a symplectic lattice resemble synchronized states in a locally dissipative lattice, we can resort to a numerical diagnostic provided by the order parameter introduced by Kuramoto [29,30],

$$Z_n = \left| \frac{1}{N} \sum_{j=1}^{N} \exp(2\pi i x_n^{(j)}) \right|^2, \tag{16}$$

for a given time n. A similar quantity, with the normalization factor $1/\sqrt{N}$ instead of $1/N$, has been called degree of clustering by Konishi and Kaneko [15]. We can interpret Z_n as the amplitude of a centroid phase vector which denotes the angular positions $2\pi x_n^{(i)}$ of particles distributed along a chain with periodic boundary conditions.

If all the states are so fully clustered that the values of $x_n^{(i)}$ are exactly the same for all times, then the superposition of phase vectors with the same amplitude at each time for all lattice sites yields $Z = 1$. On the other hand, when the site amplitudes $x_n^{(j)}$ are uniformly distributed over the lattice, the centroid phase vector amplitude vanishes and $Z = 0$. Moreover, if the positions $x_n^{(i)}$ are so uncorrelated that they can be considered as essentially random variables, one has $Z = (1/N) \ll 1$ for large N. We can define clustered motion as that for which $Z > (1/N)$. However, a handy criterion is that partially or non-clustered states correspond to low values of the order parameter ($0 < Z \lesssim 0.2$), whereas totally or nearly fully clustered states correspond to values close to the unity ($0.8 \lesssim Z < 1$).

Fig. 6 exhibits an example of clustered states in a lattice with $K = 0.1$ and $\alpha = 0$ (global coupling), for which we have chosen a phase-space projection for a fixed ($i = 10$) site. A trajectory orbits around the origin for $\sim 2 \times 10^4$ iterations and then wanders chaotically over a wider region [Fig. 6(a)]. While the trajectory orbits around the origin, the order parameter fluctuates in the interval $0.8 \lesssim Z \lesssim 0.9$, what characterizes clustered motion [Fig. 6(b)]. After the trajectory escapes, the orbital motion starts wandering erratically through the chaotic sea, and the order parameter drops to values fluctuating between 0 and 0.2, indicating absence of clustering. Essentially the same conclusions can be drawn from lattices with an almost local coupling (large α) [Fig. 7], which also exhibit clustered trajectories which eventually escape from the vicinity of remnant islands.

The origin of the orbiting behavior that generates clustering in the previous example is a well-known phenomenon in symplectic maps named *stickiness*. When a chaotic trajectory is close enough to outer quasi-periodic KAM tori belonging to island remnants embedded in the chaotic sea, it follows the orbiting nature of trajectories on tori (i.e., the chaotic trajectory sticks to the tori) [18]. Since there is no longer a KAM torus there, however, the trajectory eventually leaves this region

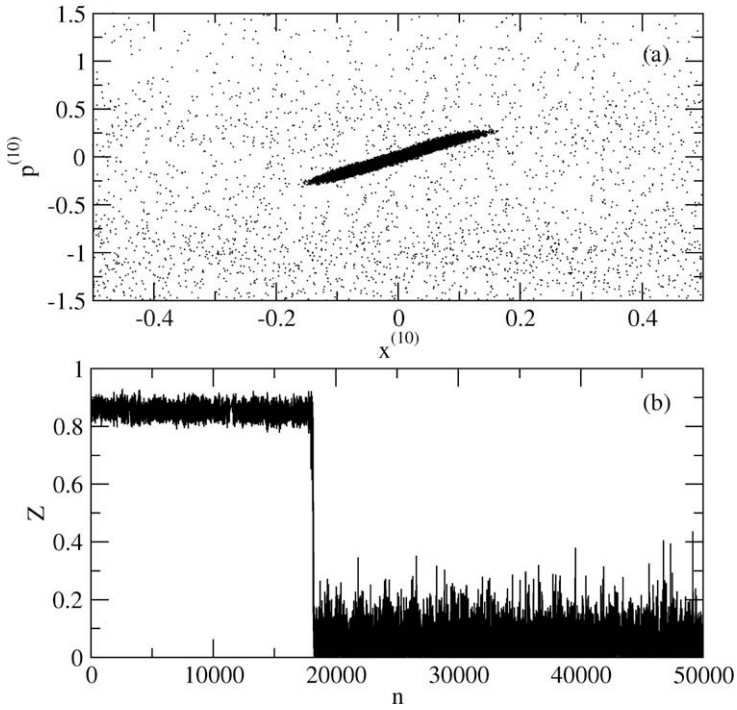

Fig. 6. (a) Phase-space projection $p^{(10)}$ *versus* $x^{(10)}$ for $K = 0.1$ and $\alpha = 0$. (b) Time evolution of the corresponding order parameter.

and wanders through the available phase-space region. In fact, the trajectories near the origin in Fig. 6(a) are orbiting around the existent tori [cf. also Fig. 2(b)]. For large K such tori occupy a small but non-zero fraction of the phase-space, and thus may not be easily detected due to insufficient numerical and/or graphical resolution. In spite of this, such tori exerts a considerable influence on chaotic motion through stickiness.

The stickiness phenomenon has been intensively studied in symplectic system with few degrees of freedom [18,19,21,22]. Stickiness of chaotic trajectories for a finite time creates a dynamical trap which is responsible for an effective transport barrier in dynamical systems of interest in plasma fusion research [31]. Our numerical results, of which Figs. 6 and 7 are representative examples, support the key hypothesis that the stickiness of chaotic trajectories to periodic island remnants manifests spatially in the form of clusters[15].

5. Diffusion

A characteristic feature of high-dimensional conservative dynamical system is the diffusion of chaotic trajectories along the energetically available phase-space. If these chaotic orbits are uniformly random, as in a gas of hard spheres, the diffusion is generally assumed to be Gaussian, or coming from a Markov process, for which there is essentially no time correlations. The possible formation of clustered states, on the other hand, introduces long-time correlations in the dynamics, since such clusters have a finite lifetime and may be considered as meta-stable states. A chaotic trajectory may be trapped for some time in such a cluster and then switch to another one, in a kind of chaotic itineracy. Such episodes make the diffusion to deviate from the normal Gaussian approximation.

One of the difficulties experienced in studying high-dimensional conservative system lies in the large timescales necessary to evidence the deviations from the Gaussian approximation due to, for example, trapping in clustered states. This is specially true for weak non-integrability, since the diffusion rate has the Nekhoroshev upper bound $\exp(-1/K^a)$, where K is the strength of non-linearity and $a > 0$. For small K the timescale involved in diffusive process can be extremely large.

In order to investigate numerically the influence of coupling parameters in the momentum diffusion rate we define the diffusion coefficient

$$D = \left\langle \lim_{n\to\infty} \frac{1}{N} \sum_{i=1}^{N} \frac{1}{n} \left[p_n^{(i)} - p_0^{(i)} \right]^2 \right\rangle, \tag{17}$$

where $\langle \cdots \rangle$ is an average taken over many initial conditions yielding independent chaotic orbits. In general the average quadratic deviation increases with time as a power-law $[p_n^{(i)} - p_0^{(i)}]^2 \propto n^{\beta+1}$, such that $\beta = 0$ characterizes the Gaussian diffusion, whereas the cases for which $\beta \neq 0$ are referred to as of anomalous diffusion. The diffusion coefficient has a stationary value in

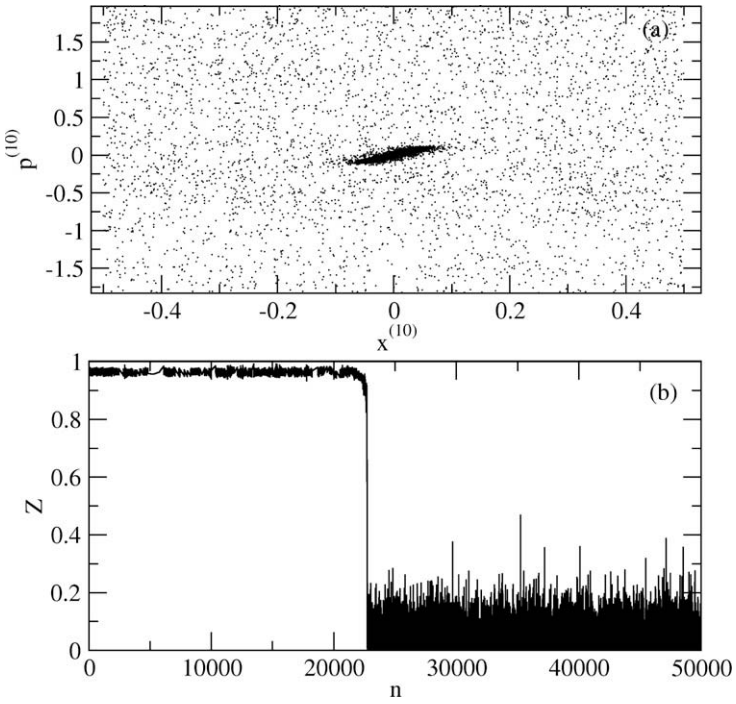

Fig. 7. (a) Phase-space projection $p^{(10)}$ *versus* $x^{(10)}$ for $K = 0.1$ and $\alpha = 6$. (b) Time evolution of the corresponding order parameter.

the former situation, whereas in the latter we can write $D \propto n^{\beta}$, where positive (negative) values of the exponent characterize super-diffusive (sub-diffusive) processes.

In the $\alpha = 0$ case of the CML, given by Eqs. (6) and (7), we can write the momentum displacement at each time as

$$\left|p_{n+1}^{(i)} - p_n^{(i)}\right|^2 = \frac{K^2}{4\pi^2(N-1)}\left|\sum_{j=1\,j\neq i}^{N} \sin\left[2\pi(x_n^{(j)} - x_n^{(i)})\right]\right|^2. \tag{18}$$

Supposing that Gaussian diffusion takes place, and assuming that the phases $x_n^{(i)}$ are so randomly distributed that they can be taken as statistically independent, we approximate the spatial average in the above equation by an ensemble average equal to 1/2 (random-phase approximation), such that one finds a quadratic dependence in K for the (quasi-linear) diffusion coefficient

$$D_{\mathrm{QL}} = \frac{K^2}{8\pi^2}. \tag{19}$$

Let us consider the more general case of arbitrary range parameter α. In Fig. 8, we follow the time evolution of the diffusion coefficient for different values of α. When $\alpha = 6$ we are practically in the local regime where only the nearest-neighbors of a given site count. Apart from small-amplitude fluctuations, the diffusion coefficient appears to have a stationary value close to that predicted by the quasi-linear value (for $K = 1$) $D_{\mathrm{QL}} \approx 0.0127$; hence Gaussian diffusion sets in for this case. For lower values of α we observe that the diffusion coefficient remains to be Gaussian but with lower stationary values. This indicates that, although the chaotic excursion of phase-space trajectories is chiefly random its time rate is lowered due to the influence of stickness. The trajectories may be trapped for some time in the neighborhood of some periodic island, leading to clustering, and this reduces the diffusion coefficient. Accordingly, lower values of the diffusion coefficient are achieved when $\alpha = 1$, when the effect of stickness and clustering are the most preeminent, as we have argued in the previous section. As we approach the $\alpha = 0$ case the diffusion coefficient increases again to a value near the quasi-linear approximation (19).

These findings are confirmed by Fig. 9, where we plotted the average diffusion coefficient $\langle D\rangle$ after some transient time is discarded (such that this average is a numerical approximation to the stationary value of D) *versus* the α parameter for a different value of the non-linearity parameter ($K = 5.0$). The stationary value of the diffusion coefficient for large α takes on values near the predicted quasi-linear limit $D_{\mathrm{QL}} \approx 0.317$ and decreases with α as before, until it reaches a minimum value for $\alpha = 1$ and resumes increasing until $\alpha = 0$. We stress the remarkable similitude between Figs. 9 and 5, what suggests a strong connection between the diffusion and entropy due to the presence of clustering and stickness.

Another sequence of numerical experiments is illustrated by Fig. 10, where we plotted the time-averaged value of the diffusion coefficient (as an approximation of its stationary value) as a function of the non-linearity parameter K and different

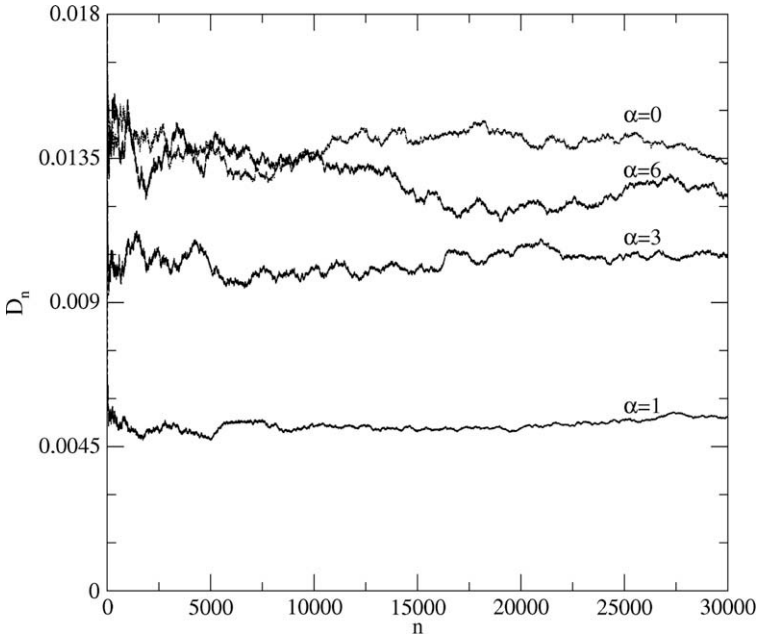

Fig. 8. Time evolution of the diffusion coefficient for a lattice of $N = 25$ coupled standard maps, with $K = 1$ and selected values of α.

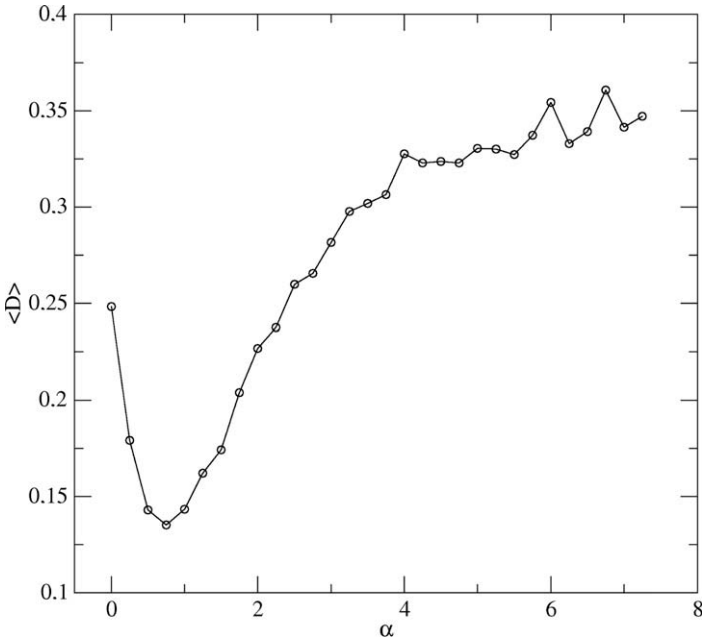

Fig. 9. Average diffusion coefficient for a lattice of $N = 25$ coupled standard maps, with $K = 5.0$, as a function of the range parameter α.

values of α. We see that in all cases considered $\langle D \rangle$ increases quadratically with K and, as we approach large values of α we have essentially the same dependence possessed by the quasi-linear approximation (19). These results are in accordance with previous findings of Konishi and Kaneko, who predicted $D \propto K^{\varpi}$, with $\varpi = 2$ for $K \gtrsim 1$ and $\varpi \sim 5$ for $K \lesssim 1$ for locally coupled lattices (the $\alpha \to \infty$ limit in our case) [13,14]. By way of contrast, the diffusion coefficient was found to increase with K as a stretched exponential $D \propto K \exp(-\xi K^{-\beta})$, where $\beta \sim 0.5$ and $\xi > 0$ for globally coupled lattices of *small sizes* (the $\alpha \to 0$) [14]. If K is large enough the exponential dependence could be neglected such that D would scale linearly with K. However, our results suggest that this almost linear dependence holds only for small values of K, at least for a lattice with $N = 25$ maps, hence substantially larger than the values (up to $N = 6$) used in Ref. [14].

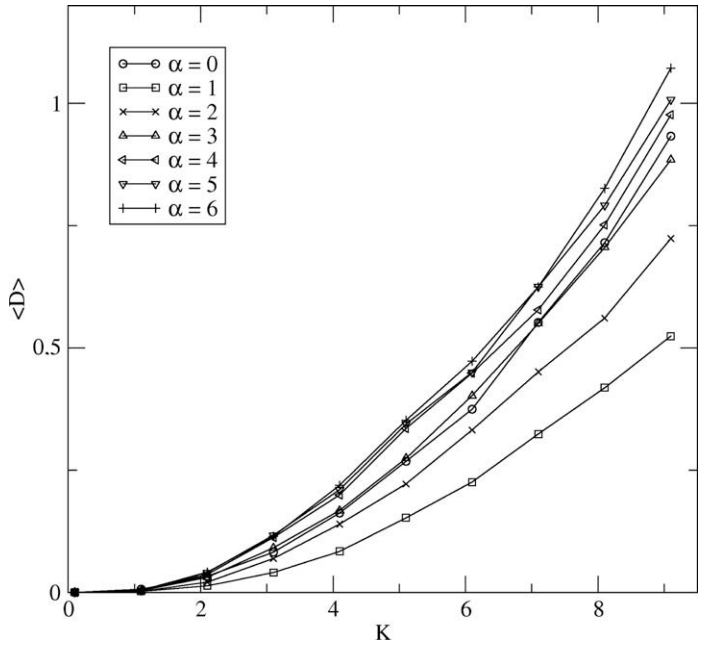

Fig. 10. Average diffusion coefficient for a lattice of $N = 25$ coupled standard maps as a function of the non-linearity parameter K for selected values of the range parameter α.

We conclude that the stickiness and clustering do not alter the Gaussian character of the diffusion of phase-space trajectories process but only its time rate, lowering the stationary values achieved by the diffusion coefficient. This is compatible with the picture we made of trajectories being trapped for some time in the neighborhood of islands and then reinjected in the energetically available chaotic region. Anomalous diffusion can be exist only up to some crossover time (inversely proportional to the diffusion coefficient), beyond which the diffusion is Gaussian [13].

6. Approximate two-dimensional map

Since we have focused on the clustering phenomenon related to the stickiness of the trajectory around the origin (0,0), we can study the properties of this orbiting behavior by obtaining an approximate form of the system in that region. We can rewrite Eqs. (1) and (2) in the following form

$$p_{n+1}^{(i)} = p_n^{(i)} + \mathscr{F}_n^{(i)}(\mathbf{x}_n), \tag{20}$$

$$x_{n+1}^{(i)} = x_n^{(i)} + p_{n+1}^{(i)}, \tag{21}$$

where

$$\mathscr{F}_n^{(i)}(\mathbf{x}_n) \equiv \frac{K}{2\pi\sqrt{\eta(\alpha)}} \sum_{j=1}^{N'} \frac{1}{j^\alpha} \left\{ \sin\left[2\pi(x_n^{(i+j)} - x_n^{(i)})\right] + \sin\left[2\pi(x_n^{(i-j)} - x_n^{(i)})\right] \right\} \tag{22}$$

is a time-dependent coupling term which depends on the values of all site amplitudes. If the trajectories are near the origin both $x_n^{(i)}$ and $p_n^{(i)}$ take on small values and we can approximate the coupling term as follows

$$\mathscr{F}_n^{(i)}(\mathbf{x}_n) \approx -C_2 x_n^{(i)} + C_1 \sum_{j=1}^{N'} \frac{x_n^{(i+j)} + x_n^{(i-j)}}{j^\alpha}, \tag{23}$$

where we define

$$C_1 \equiv \frac{K}{\eta(\alpha)}, \quad C_2 = \eta(\alpha) C_1. \tag{24}$$

For large α the normalization factor $\eta^{-1/2}$ remains constant at a value of $\sim$0.9 regardless of the lattice size. In general, the factor decreases with as N grows up, and for the extreme case of $\alpha = 0$ it tends to a value of $\sim$0.1. Hence a "safe" interval for the variation of this factor is [0,0.8], which means that $\eta \gtrsim 1.56$. If η is large enough, it may follow that C_2 is much larger than C_1 and thus we can also neglect the summation term in the coupling term (23). In such cases the system can be approximately described by a two-dimensional area-preserving map

$$p_{n+1}^{(i)} = p_n^{(i)} - C_2 x_n^{(i)}, \tag{25}$$

$$x_{n+1}^{(i)} = x_n^{(i)} + p_{n+1}^{(i)}, (\text{mod } 1), \tag{26}$$

which has the origin (0,0) as its only fixed point, whose stability is determined by the eigenvalues of its Jacobian matrix, namely

$$\xi_{1,2} = \frac{2 - C_2}{2} \pm \mathrm{i}\sqrt{1 - \left(\frac{2 - C_2}{2}\right)^2}, \tag{27}$$

such that (0,0) is a linear center inasmuch $C_2 < 4$. Within this approximation, the values of $(x_n^{(i)}, p_n^{(i)})$ are assumed to be close to the elliptic fixed points of the coupled map lattice.

Some phase portraits obtained through iterating the piecewise linear map above are shown in Fig. 11(a)–(d) for different values of the parameter C_2. For $C_2 < 4$ the fixed point is a linear center, the trajectories encircling it in its neighborhood [Fig. 11(a) and (b)]. When $C_2 = 4$ there occurs a bifurcation and the origin becomes an unstable saddle point [Fig. 11(c)]. When $C_2 > 4$ this point becomes embedded into a chaotic orbit, which is possible thanks to the modulo 1 prescription present in Eq. (26) [Fig. 11(d)] (the map is actually piecewise linear).

These results can be compared with those shown in Fig. 12(a)–(d), where we plot the phase-space projection $p(10)$ *versus* $x(10)$ of the coupled SM lattice (1) and (2) for $\alpha = 0$ and selected values of K. For smaller K-values chaotic trajectories exhibit sticky behavior, during a given time, while remaining near to the fixed point at origin [Fig. 12(a) and (b)], and are approximately described by the closed trajectories encircling the origin in the piecewise linear map (25) and (26) when C_2 is small enough. We stress, however, that stickiness is a transient phenomenon in the coupled SM lattice and thus this analogy cannot be pushed too far, since in the two-dimensional map the iterations are bound to closed orbits for all further times.

When K is close to $K_c \approx 0.86$ it appears that the origin is undergoing a change of stability, the sticky orbits being more flattened into the diagonal of the phase-space projection shown [Fig. 12(c)]. Finally, for $K > K_c$, it turns out that the dynamics near the origin is chaotic for the coupled SM lattice [Fig. 12(d)], just like it occurs for the piecewise linear map [see also Fig. 11(d)]. Comparing the results obtained with the coupled SM lattice with those for the piecewise linear map, we can relate the critical K-value for the loss of stability of the origin for the CML with the similar transition observed in the two-dimensional map, the latter occurring for $(C_2)_{\text{crit}} = 4$, such that

$$K_c = \frac{4}{\sqrt{\eta}}, \tag{28}$$

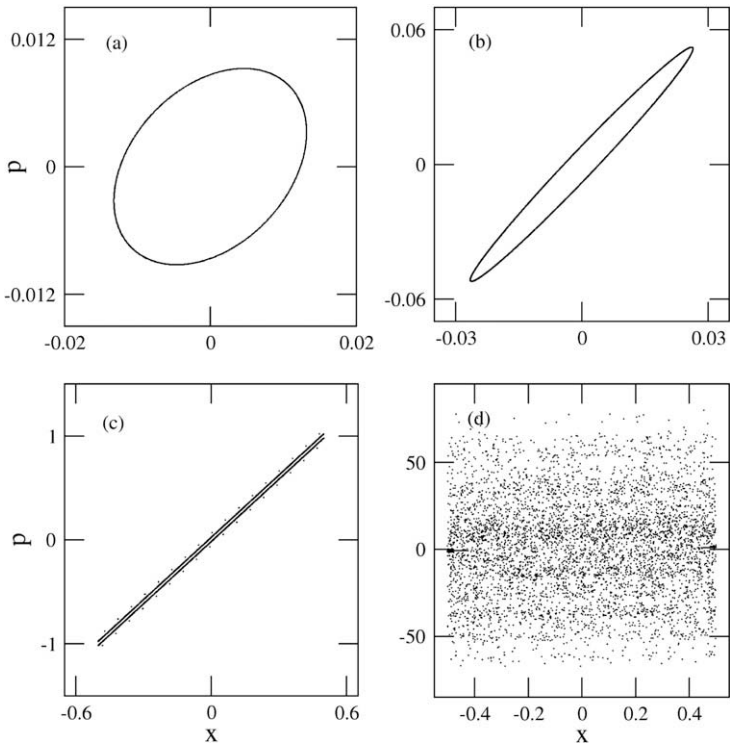

Fig. 11. Phase portraits of the piecewise linear map (25) and (26) for $C_2 =$ (a) 2.0; (b) 3.5; (c) 4.0; (d) 5.0.

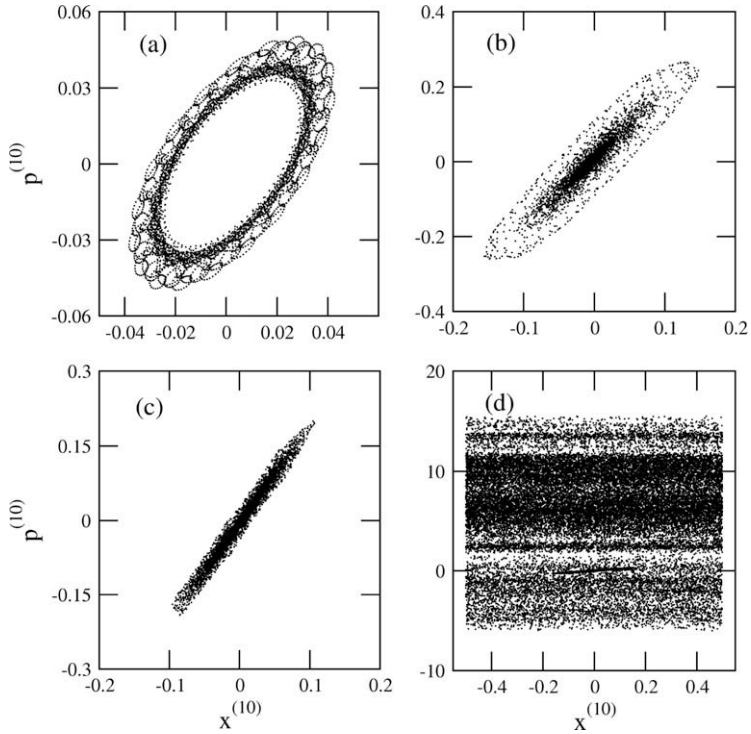

Fig. 12. Phase-space projection $p^{(10)}$ *versus* $x^{(10)}$ for $\alpha = 0$ and $K =$ (a) 0.3; (b) 0.8; (c) 0.86; and (d) 1.0. In all figures there is one orbit with 5×10^4 points starting from the initial condition $x_0^{(10)} = -0.023, p_0^{(10)} = -0.033$.

where we also used Eq. (24). For a lattice of fixed size there follows that, in the limits of local (nearest-neighbor) and global (mean-field) couplings, this critical value is given by

$$K_c = \begin{cases} 4/\sqrt{N-1} & \text{if } \alpha = 0, \\ \sqrt{8} & \text{if } \alpha \to \infty. \end{cases} \tag{29}$$

In fact, for $\alpha = 0$ and $N = 25$ maps, as considered in Fig. 12, there results that $K_c = 0.816$ which is close to the value guessed by inspecting Fig. 12(c). On the other hand, if we consider a locally coupled lattice, as in Fig. 13, there results that $K_c = 2.828$ for the same number of maps, which is twice the actual value of 1.45 which comes from analyzing the situation depicted in Fig. 13(c). Figs. 13(a), (b), and (d) represent cases for which K is less and greater than K_c, respectively. This discrepancy is due to the breakup of the approximation represented by the piecewise linear map with respect to the actual coupled SM lattice.

7. Conclusions

We have considered a conservative chain of standard maps with a non-local coupling for which the interaction strength decays with the lattice distance as a power-law. The limiting cases of local and global couplings were previously considered in Refs. [13,14] as paradigmatic examples of Hamiltonian systems with a large number of degrees of freedom, and more easily tractable from the computational point of view than physical systems appearing in statistical mechanical or astronomical contexts. Our work represents a step towards generalizing such treatment to Hamiltonian systems with long-range interactions, such as gravitational or electromagnetic forces, which naturally lead to an inverse power-law dependence for the potential energy.

Non-integrable Hamiltonian systems of physical interest, although presenting chiefly chaotic phase-space trajectories, are strongly influenced by non-chaotic orbits. There are ordered phases, or clusters, with spatially coherent behavior, even though the time behavior may be chaotic. Such clusters have a finite lifetime, since the chaotic trajectories are free to eventually wander through a large energetically accessible portion of the phase-space, the latter being spatially incoherent. We have analyzed the dependence of the chaotic instability with the coupling parameters, and observed an enhanced chaotic diffusion in globally coupled lattices, when compared with couplings with smaller effective interaction range. We also found that, for some coupling ranges there is a decrease of the chaotic instability, which we related to the existence of clusters.

We have provided numerical evidence that the underlying mechanism of clustering is the stickiness of the chaotic trajectories close enough to remnants of periodic islands embedded in the chaotic sea. An approximate low-dimensional map was

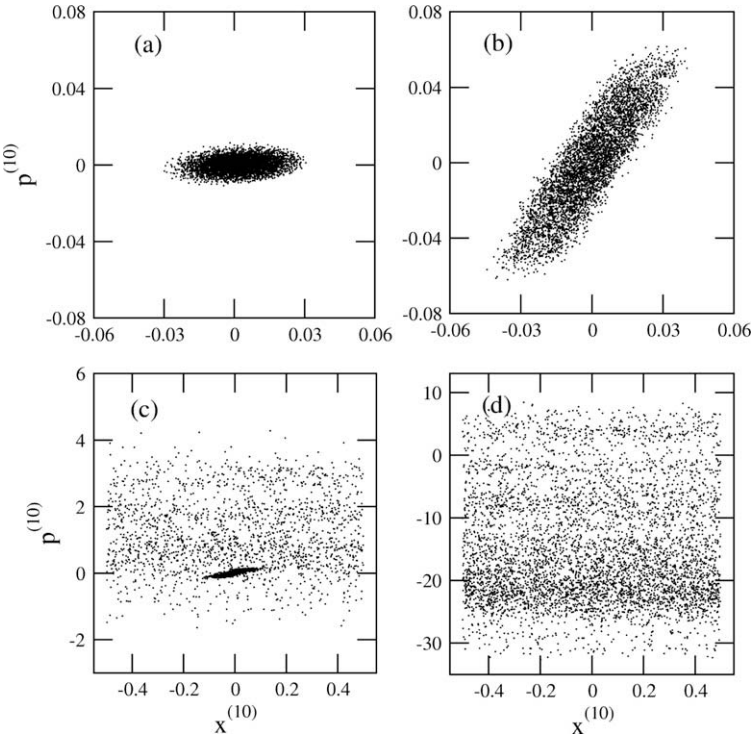

Fig. 13. Phase-space projection $p^{(10)}$ *versus* $x^{(10)}$ for $\alpha = 6$ and $K =$ (a) 0.7; (b) 1.4; (c) 1.5; and (d) 1.7. In all figures there is one orbit with 5×10^4 points starting from the initial condition: $x_0^{(10)} = -0.013, p_0^{(10)} = -0.033$.

derived to investigate this relation. We found that stickiness ceases when the global fixed point of the coupled map lattice becomes unstable, what occurs for a critical value of the coupling strength. In terms of our low-dimensional map this corresponds to a bifurcation, from which we were able to predict correctly the critical value of the coupling strength for the loss of stickiness in the global coupled lattice. For local coupling this approximate description shows different results, what indicates that the low-dimensional approximation is better as the effective interaction range increases.

The connection between stickiness and clustering, which was the main point of this paper, has also other consequences for the spatio-temporal dynamics of the coupled map lattice. We also verified that the behavior of the phase-space diffusion is influenced by clustering in a similar way as the Lyapunov spectrum, with respect to variations of the coupling parameters. The diffusion process remains to be essentially Gaussian such that there is a stationary value of the diffusion coefficient which, for local couplings, takes on a value close to that predicted by random-phase approximation. As the range parameter decreases and clustering becomes significant, the diffusion rate is lowered and achieves a minimum at $\alpha = 1$, similarly to the behavior observed for the entropy. The trapping effect caused by the chaotic region immediately near the periodic islands causes a retardation of the diffusion process without altering its non-anomalous character. Finally, we conjecture that the different timescales present in diffusion phenomena can explain the existence of stable and meta-stable spatial structures present in the phase-space, which is a relevant investigation for prospective applications in statistical mechanics and astronomy.

Acknowledgements

This work was made possible by partial financial support from the following Brazilian government agencies: CNPq, CAPES, FAPESP, and Fundação Araucária. The numerical computations were performed in the NAUTILUS cluster of the Universidade Federal do Parana.

References

[1] Chirikov BV. Phys Rep 1979;52:263.
[2] Rechester AB, White RB. Phys Rev Lett 1980;44:1586.
[3] Schmidt G. Phys Rev A 1980;22:2849.
[4] Rechester AB, Rosenbluth MN. Phys Rev Lett 1978;40:38;
Rechester AB, Rosenbluth MN, White RB. J Phys 1980;41:C3–C351.
[5] Rosenbluth MN, Sagdeev RZ, Taylor JB, Zaslavsky GM. Nucl Fusion 1966;6:297.
[6] Zaslavsky GM, Chirikov BV. Usp Fiziol Nauk 1972;14:195 [Sov Phys Usp 1972;114:549].

[7] Caglioti E, Trillo S, Wabnitz S. Opt Lett 1987;12:1044.
[8] Milburn GJ, Dyrting S. Philos Mag B 2000;80:2023.
[9] Abel M, Flash S, Pikowsky A. Phys D 1988;119:4.
[10] Lichtenberg AJ, Lieberman MA. Regular and chaotic motion. Berlin, Heidelberg, New York: Springer Verlag; 1992.
[11] Nekhoroshev NN. Russ Math Surv 1977;32:65.
[12] Bennetin G, Gallavotti G. J Stat Phys 1986;44:293.
[13] Kaneko K, Konishi T. Phys Rev A 1989;40:6130.
[14] Konishi T, Kaneko K. J Phys A 1990;23:L715.
[15] Konishi T, Kaneko K. J Phys A 1992;25:6283.
[16] Kaneko K, Konishi T. Phys D 1994;146.
[17] Gyorgyi G, Ling FM, Schmidt G. Phys Rev A 1989;40:5311.
[18] Zaslawsky GM, Edelman M, Niyazov BA. Chaos 1997;7:159.
[19] Zaslawsky GM, Edelman M. Phys Rev E 2005;72:036204.
[20] Szezech Jr JD, Lopes SR, Viana RL. Phys Lett A 2005;335:394.
[21] Barash O, Dana I. Phys Rev E 2005;71:036222.
[22] Zaslawsky GM. Phys Rep 2002;371:461.
[23] Kaneko K. Phys Rev Lett 1989;63:219;
Kaneko K. Phys Rev Lett 1989;65:1391;
Kaneko K. Phys D 1990;41:137.
[24] Rogers JL, Wille LT. Phys Rev E 1996;54:R2193.
[25] Carretero-González R, Ørstavik S, Huke J, Broomhead DS, Stark J. Chaos 1999;9:466.
[26] Pesin YB. Russ Math Surv 1977;32:55.
[27] Ruelle D. Chaotic evolution and strange attractors. Cambridge: Cambridge University Press; 1989.
[28] Bricmont J, Kupiainen A. Phys D 1997;103:18.
[29] Kuramoto Y. Chemical oscillations waves and turbulence. Berlin, Heidelberg, New York: Springer Verlag; 1984.
[30] de Souza Pinto SE, Viana RL. Phys Rev E 2000;61:5154.
[31] Roberto M, da Silva EC, Caldas IL, Viana RL. Phys Plasmas 2004;11:214.